The Journal of Immunology

Guanylate Binding Protein 4 Negatively Regulates Virus-Induced Type I IFN and Antiviral Response by Targeting IFN Regulatory Factor 7

Yu Hu, Jie Wang, Bo Yang, Nuoyan Zheng, Meiling Qin, Yongyong Ji, Guomei Lin, Lin Tian, Xiaodong Wu, Li Wu and Bing Sun

J Immunol 2011; 187:6456-6462; Prepublished online 16 November 2011;
doi: 10.4049/jimmunol.1003691
http://www.jimmunol.org/content/187/12/6456

The Journal of Immunology is published twice each month by
The American Association of Immunologists, Inc.,
1451 Rockville Pike, Suite 650, Rockville, MD 20852

Print ISSN: 0022-1767 Online ISSN: 1550-6606.

Guanylate Binding Protein 4 Negatively Regulates Virus-Induced Type I IFN and Antiviral Response by Targeting IFN Regulatory Factor 7

Yu Hu,*,[1] Jie Wang,*,[1] Bo Yang,* Nuoyan Zheng,[†,‡] Meiling Qin,* Yongyong Ji,* Guomei Lin,* Lin Tian,* Xiaodong Wu,* Li Wu,[†,‡] and Bing Sun*,[§]

IRF7 is known as the master regulator in virus-triggered induction of type I IFNs (IFN-I). In this study, we identify GBP4 virus-induced protein interacting with IRF7 as a negative regulator for IFN-I response. Overexpression of GBP4 inhibits virus-triggered activation of IRF7-dependent signaling, but has no effect on NF-κB signaling, whereas the knockdown of GBP4 has opposite effects. Furthermore, the supernatant from Sendai virus-infected cells in which GBP4 have been silenced inhibits the replication of vesicular stomatitis virus more efficiently. Competitive coimmunoprecipitation experiments indicate that overexpression of GBP4 disrupts the interactions between TRAF6 and IRF7, resulting in impaired TRAF6-mediated IRF7 ubiquitination. Our results suggest that GBP4 is a negative regulator of virus-triggered IFN-I production, and it is identified as a novel protein targeting IRF7 and inhibiting its function. ***The Journal of Immunology*****, 2011, 187: 6456–6462.**

Innate immunity is the first line of host defense against viral infection. The interaction of viral pathogen-associated molecular patterns and pattern-recognition receptors is crucial for initiating the innate immune response that is sufficient to clear viral infection (1–3). Among pattern-recognition receptors, TLR3 recognizes the genomic RNA of reoviruses and dsRNA produced during the replication of ssRNA (4, 5). TLR7 (mouse) and TLR8 (human) recognize ssRNA of RNA viruses (6, 7). TLR9 serves as a sensor of DNA virus infection (e.g., CMV, HSV1, HSV2) (8–10). Unlike TLRs, *RIG-I*–like helicases (RLHs; including *RIG-I* and *MDA-5*) (11, 12) are cytoplasmic sensors of virally derived dsRNA. RLHs share caspase recruitment domains at their N terminus followed by a DexD/H-box helicase domain at the C terminus, which recognize intracellular RNA through the helicase domains and transmit signals to downstream virus-induced signaling adaptor (VISA; also known as IPS-1, MAVS, and Cardif) via the caspase recruitment domain. VISA, then providing an interface for direct binding to and activation of the TNF receptor-associated factor (TRAF) family members (TRAF3 and TRAF6), in turn activates the inhibitor of NF-κB kinase (IKK) α-β-γ complex and the TBK1 inducible IKKs (IKKi), thus provoking activation of NF-κB and IFN regulatory factor (IRF). Thus, engagement of any of those pattern-recognition receptors triggers rapid production of type I IFN, which causes suppression of viral replication, clearance of virus, and facilitation of an adaptive immune response (13, 14).

Induction of type I IFNs critically depends on IRF3 and IRF7. IRF3 is activated by C-terminal phosphorylation, which promotes dimerization, cytoplasmic to nuclear translocation, and transactivation of downstream early genes such as IFN-β and IP-10. In contrast, IRF7, the master regulator of production of type I IFN, is synthesized upon IFN stimulation and contributes to the expression of IFN-α and delayed type genes (15). Similar to IRF3, virus infection induces C-terminal phosphorylation and activation of IRF7. Until now, many kinds of factors have been found to negatively regulate IRF3-dependent signaling (16–19); however, the molecular mechanisms for the regulation of IRF7 remain to be further identified.

Guanylate binding protein (GBP) 4 belongs to a group of IFN-inducible GTPase families, including the p47 GBP family, the p65 GBP family, Mx, and very large inducible GTPase (20, 21). The p65 GBP family has 13 members, GBP1 to GBP13, sharing common structural features including an N terminal GTP binding domain and the common biochemical property of oligomerization-

*Laboratory of Molecular Cell Biology, Institute of Biochemistry and Cell Biology, Shanghai Institutes for Biological Sciences, Chinese Academy of Sciences, Shanghai 200031, China; [†]Tsinghua University–Peking University Joint Center for Life Sciences, Beijing 100084, China; [‡]Tsinghua University School of Medicine, Beijing 100084, China; and [§]Molecular Virus Unit, Key Laboratory of Molecular Virology and Immunology, Institute Pasteur of Shanghai, Chinese Academy of Sciences Shanghai 200025, China

[1]Y.H. and J.W. contributed equally to this work.

Received for publication November 5, 2010. Accepted for publication September 23, 2011.

This work was supported by grants from the Chinese Academy of Sciences (KSCX2-YW-R-161, KSCX2-YW-R-169, and KSCX2-EW-J-14), the National Ministry of Science and Technology (2007DFC31700), the National Natural Science Foundation of China (30950002, 30623003, 30721065, 30801011, 30870126, 31030029, and 90713044), the National Science and Technology Major Project (2009ZX10004-016, 2008ZX10004-002, and 2009ZX10004-105), the National 973 Key Project (2007CB512404), the Shanghai Pasteur Health Research Foundation (SPHRF2008001 and SPHRF2009001), the National 863 Project (2006AA02A247), and the Li Kha Shing Foundation. L.W. was supported by a grant from the Tsinghua-Yu Yuan Foundation (20200584), a Janssen Investigator award, and a 985 Grant from Tsinghua University.

The microarray data presented in this article have been submitted to the Gene Expression Omnibus (http://www.ncbi.nlm.nih.gov/geo/query/acc.cgi?token=jhcpxwgmegacwfa&acc=GSE32499) under accession numbers GSE32499, GSM804441, and GSM804442.

Address correspondence and reprint requests to Dr. Bing Sun or Dr. Li Wu, Laboratory of Molecular Cell Biology, Institute of Biochemistry and Cell Biology, Shanghai Institutes for Biological Sciences, Chinese Academy of Sciences, 320 Yue Yang Road, Shanghai 200031, China (B.S.) or Tsinghua University School of Medicine, Shuang Qing Road, Beijing 100084, China (L.W.). E-mail addresses: bsun@sibs.ac.cn (B.S.) and wuli@tsinghua.edu.cn (L.W.)

The online version of this article contains supplemental material.

Abbreviations used in this article: BMDC, bone marrow derived dendritic cell; GBP, guanylate binding protein; HA, hemagglutinin; HAU, hemagglutinating unit; IKK, inhibitor of NF-κB kinase; IKKi, inducible IKK; IRF, IFN regulatory factor; RIG-I, retinoic acid-inducible gene I; RLH, *RIG-I*–like helicase; SeV, Sendai virus; TRAF, TNF receptor-associated factor; VISA, virus-induced signaling adaptor; VSV, vesicular stomatitis virus.

dependent GTPase activity (22). To date, few studies have investigated the function of distinct GBPs. GBP1, which is the first cloned member of the p65 GBP family, was reported to mediate antiviral effects against vesicular stomatitis virus (VSV), encephalomyocarditis virus and hepatitis C virus (23, 24). GBP2 exerts a similar effect against encephalomyocarditis virus (25); however, the function of the other members is less well characterized.

In this report, we present evidence that GBP4 disrupts the interaction of TRAF6 with IRF7, resulting in an impaired IFN-α expression. Our results define a novel mechanism controlling type I IFN induction by targeting IRF7.

Materials and Methods

CDNA constructs and reagents

Mouse GBP4 (NP_061204), IRF7 (NP_058546), IRF3 (NP_058545), Ikki (NP_062751), and TRAF3 (NP_035762) were amplified by PCR using cDNA from Sendai virus (SeV)-infected bone marrow-derived dendritic cells (BMDCs) and cloned into pcDNA3 (Invitrogen). All IRF7 and GBP4 deletion mutants were constructed using PCR and were subcloned into pcDNA3. Human GBP1 was cloned from IFN-α–treated Huh7 cells. FR-luc (Stratagene), pCMV-BD (Clontech), NF-κB promotor, and Flag-tagged VISA were donated by Chen Wang (Shanghai Institutes for Biological Sciences, Shanghai, China). PCMV-BD-IRF7 was constructed using PCR and cloning of full-length IRF7 into pCMV-BD. The reporter constructs of mouse IFN-α4 and IFN-α6 were generated as described previously (26). The FLAG-tagged RIG-I plasmid was obtained from Takashi Fuijita (Institute for Virus Research, Kyoto University, Kyoto, Japan). Vesicular stomatitis virus was provided by Hongbing Shu (Wuhan University, Wuhan, China). The constructs for TRAF6 and TBK1 were generated as previously described (27). Anti-hemagglutinin (HA) was obtained from Covance (HA.11, 16B2, CO-MMS-101R) and anti-FLAG (M2, F3165) from Sigma. Polyclonal rabbit anti-mouse IRF7 and GBP4 Abs were raised against recombinant mouse GBP4 (120-597) and IRF7 (full length), respectively (The Ab Research Center, Shanghai Institutes for Biological Sciences). SeV (250 hemagglutinating units [HAU] per milliliter) was provided by Wuhan Institutes of Virology, Chinese Academy of Sciences.

Cells

Hek293T and Raw264.7 were cultured in DMEM. L929 cells were grown in RPMI 1640. All cells were supplemented with 10% FBS (Invitrogen), 4 mM L-glutamine, 100 U/ml penicillin, and 100 U/ml streptomycin under humidified conditions with 5% CO_2 at 37°C. BMDCs were generated as described previously (28). Hek293T cells was transfected with Lipofectamine (Invitrogen). Raw264.7 was transfected using Lipofectamine 2000 (Invitrogen) according to the manufacturer's instructions.

Infection

Hek293T, Raw264.7, and BMDCs were incubated with 10 HAU/ml of SeV in serum-free medium for 2 h and then combined with the same volume of medium containing 20% FBS. After infection, cells were collected and used for various experiments.

Immunoprecipitation and immunoblot analysis

Immunoprecipitation and immunoblot analysis were performed as described previously (27). Hek293T cells were transfected with various combinations of plasmids. At 24 h after transfection, cell lysates were prepared in lysis buffer and incubated with indicated Ab together with protein A/G Plus-Agarose Immunoprecipitation reagent (Santa Cruz) at 4°C for 3 h or overnight. After three washes, the immunoprecipitates were boiled in SDS sample buffer for 10 min and analyzed by immunoblotting. For ubiquitination, HEK293T cells were transfected with GFP-IRF7 together with Flag-TRAF6, HA-ubiquitin, and indicated plasmids. Next, proteins were immunoprecipitated with anti-GFP, followed by immunoblotting with anti-HA and anti-GFP. For endogenous coimmunoprecipitation experiments, Raw264.7 cells (2×10^7) were infected with 10 HAU/ml SeV for 12 h, and then cell lysates were prepared in lysis buffer and incubated with 1 μl preimmune serum or antiserum against GBP4. The subsequent procedures were completed as described above.

Luciferase assay

Hek293T and Raw264.7 were transfected with reporter plasmids, Renilla luciferase plasmids as an internal control, and the indicated expressing plasmids. The total DNA concentration was kept constant by supplementing with empty vector pcDNA3.0. At 24 h after transfection, cells were lysed in passive lysis buffer or infected with 10 HAU/ml for an additional 24 h and lysed. The luciferase activity in the lysates was analyzed by a dual luciferase reporter assay system (Promega).

Nuclear extracts

Nuclear extracts were prepared as described previously (29). Cells were harvested and washed with PBS. Cells were lysed with buffer A, which contained 10 mM HEPES, 1.5 mM MgCl2 • 6 H_2O, 10 mM KCl (pH 7.9). Before lysis, it was supplemented with 0.5 mM DTT, 1 mM PMSF, 10 μg/ml leupeptin, and aprotinin containing 0.1% Nonidet P-40. Lysate was placed on ice for 10 min and centrifuged at 10,000 rpm for 5 min at 4°C to remove cytoplasmic proteins. Nuclear proteins were extracted from the pellet in ice-cold buffer C (20 mM HEPES, 1.5 mM MgCl2 • 6 H_2O, 0.42 M NaCl, 0.2 mM EDTA, 25% glycerol [pH 7.9]; before its use, 0.5 mM DTT, 1 mM PMSF, and 10 μg/ml leupeptin and aprotinin were added). Insoluble material was removed by centrifugation at 10,000 rpm for 5 min at 4°C. Protein concentration was measured with the BCA protein assay reagent kit according to the manufacturer's instructions.

GBP4 SiRNA synthesis and transfection

GBP4-Stealth-RNAi (SP, 5′-UGGAAGCCAUAAGGAUUCUUGAGCA-3′; AS, 5′-UGCUCAAGAAUCCUUAUGGCUUCCA-3′), was designed by Invitrogen BLOCK-iT RNAi Designer. The negative control siRNA was obtained from Invitrogen (catalog no. 12935-200). Raw264.7 was transfected with siRNA using Lipofectamine 2000 according to the manufacturer's instructions. At 24 h after transfection, cells were used for additional experiments.

Reverse transcription and real-time PCR

Total RNA was extracted from cultured cells with TRIzol (Invitrogen) according to the manufacturer's instructions. Oligonucleotide priming and M-MLV reverse transcriptase (Invitrogen) were used for reverse transcription of purified RNA. All gene transcripts were quantified by quantitative PCR with SYBR Green QPCR Master Mix and a 7900HT Fast Real-Time PCR System (Applied Biosystems). The relative fold induction was calculated with the $2^{-\Delta\Delta}$ CT method.

Primers for PCR are listed as follows: HPRT sp 5′-GCCCTTGACTATAATGAG-3′, HPRT as 5′-GATAAGCGACAATCTACC-3′; IFN-α sp, 5′-ATGGCTAGRCTCTGTGCTTTCCT-3′; IFN-α as, 5′-AGGGCTCTCCAGAYTTCTGCTCTG-3′; IFN-α1 sp, 5′-GCCTTGACACTCCTGGTACAAATGAG-3′; IFN-α1 as, 5′-CAGCACATTGGCAGAGGAAGACAG-3′; IP-10 sp 5′-TTGCCCTTGGTCTTCTG-3′; IP-10 as 5′-GTCGCACCTCCACATAGC-3′; TNF-α sp, AGTGTCAGAAGCTCCTGTGGC-3′; TNF-α as, TGAGGCAGTATTCAAGCCTCC-3′.

IFN bioassay

The IFN bioassay was performed as described previously (30). Conditioned supernatants from SeV infected cells were overlaid onto L929 cells seeded in a 48-well plate. After 24 h, the L929 cells were infected with the IFN-sensitive VSV at a multiplicity of infection of 0.1 for 2 h in serum-free medium and then washed twice to remove resident VSV before replacing the medium. At 24 h after infection, the supernatant was subjected to plaque assay.

Plaque assay

L929 cells were used in the plaque assay. The monolayers of L929 cells were infected with 10-fold dilutions of virus stock for 2 h and overlaid with 0.8% agarose in RPMI 1640 containing 1% FBS. After incubation for 48 h at 37°C, 5% CO_2 in a humidified incubator, cells were fixed with 4% paraformaldehyde and then stained with 1% crystal violet. Numbers of plaques were counted to calculate the viral titer.

Statistics

All data are presented as the mean ± SD from at least three independent experiments. Statistical comparisons between different treatments were performed using the unpaired Student t test, where $p < 0.05$ was considered statistically significant.

Accession codes

GEO: microarray data, GSE32499 (series), and GSM804441 and GSM804442 (specific array files); available at: http://www.ncbi.nlm.nih.gov/geo/query/acc.cgi?token=jhcpxwgmegacwfa&acc=GSE32499.

Results

GBP4 is induced by SeV infection

A microarray analysis showed that SeV-infected BMDCs had highly expressed GBP4. To confirm this finding, we generated a polyclonal Ab against a fragment (120–597) of mouse GBP4. Immunoblot assays indicated that the Ab specifically recognized the mouse GBP4 protein exogenously expressed in Hek293T cells, whereas no cross-reaction with human GBP1 occurred (Fig. 1*A*). In agreement with the cDNA array data, endogenous GBP4 protein was markedly upregulated after SeV infection in both the Raw264.7 cell line, BMDCs, and plasmacytoid dendritic cells (Fig. 1*B*, Supplemental Fig. 1). The expression of GBP4 in lungs was induced in SeV-infected mice, and the expression time course coincided with decline in IFN expression in the bronchoalveolar lavage fluid of infected mice (Supplemental Fig. 2). These data collectively indicate that GBP4 is induced by SeV infection. The tissue distribution of GBP4 expression, assessed by immunoblot analysis, showed that the organs of the immune system, such as spleen and lymph nodes, displayed a high level of expression of GBP4 (Fig. 1*C*), which may indicate that the major function of GBP4 focuses on immune system.

IRF7 interacts with GBP4

Because the proinflammatory cytokines (NF-κB signaling) and type I IFNs (i.e., IFN-sensitive response element [ISRE] signaling) are essential to initiating immune response against virus infection, and based on the finding that GBP4 was highly induced by SeV-infected cells, we asked whether GBP4 has a function in the regulation of virus induced signaling. In our preliminary experiments, we found that the overexpression of GBP4 inhibited SeV-induced activation of ISRE, but did not have an effect on NF-κB promotor activation (data not shown). To explore the role of GBP4 in virus-induced ISRE signaling, we tested whether GBP4 was able to interact with the signaling molecules, which are mainly involved in virus induced activation of ISRE. We transfected Hek293T cells with expression plasmids of HA-tagged GBP4 and Flag-tagged signaling molecules (including RIG-I, VISA, TRAF3, TRAF6, TBK1, IKKi, IRF3, and IRF7) which are involved in SeV-induced activation of ISRE. Subsequent coimmunoprecipitation experiments were performed to identify the interaction between GBP4 and the other molecules. Our data show that only IRF7 bound to

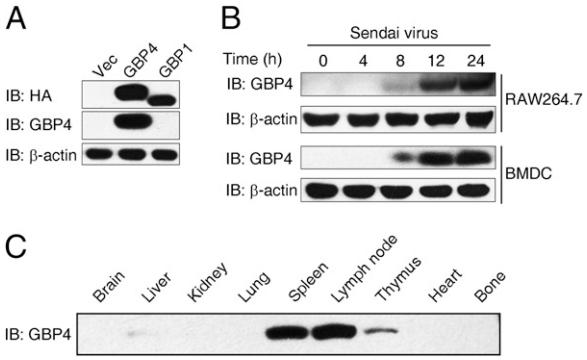

FIGURE 1. GBP4 is induced by SeV. *A*, Immunoblot of lysates of Hek293T cells transfected with HA-tagged GBP4, hGBP1 (human GBP1), or empty vector, analyzed with polyclonal anti-GBP4 or anti-HA or anti-β-actin (loading control). *B*, Immunoblot of lysates of Raw264.7 (*top*) or BMDCs (*bottom*) infected with SeV for 0–24 h, analyzed with polyclonal anti-GBP4 or anti–β-actin (loading control). *C*, Immunoblot of mouse tissue samples, quantified by bicinchoninic acid assay (30 μg protein loaded per sample), analyzed with polyclonal anti-GBP4. Data are representative of three independent experiments.

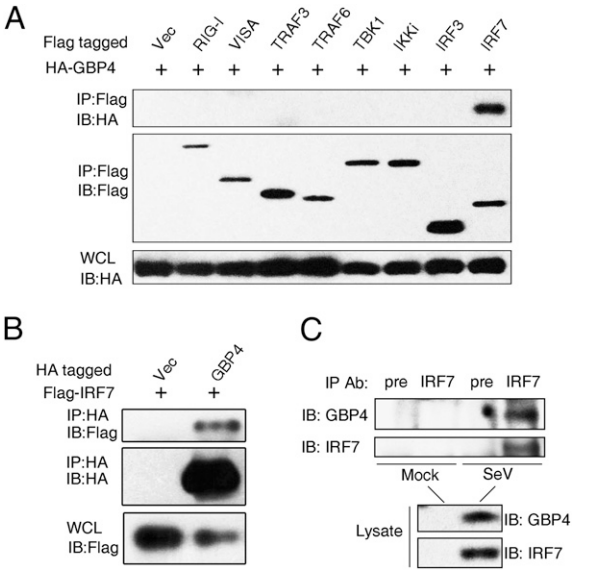

FIGURE 2. GBP4 interacts with IRF7. *A*, Hek293T cells were transfected with HA-tagged GBP4 and empty vector (Vec) or indicated Flag-tagged plasmids. Cell lysates were immunoprecipitated (IP) with anti-Flag, and the immunoprecipitates were analyzed by immunoblot (IB) with anti-HA or anti-Flag. Whole cell lysates (WCLs) were analyzed by IB with anti-HA. *B*, Hek293T cells were transfected with Flag-tagged IRF7 and empty vector (Vec) or HA-tagged GBP4. Cell lysates were IP with anti-HA and the immunoprecipitates were analyzed by IB with anti-HA or anti-Flag. WCLs were analyzed by IB with anti-Flag. *C*, Interaction between endogenous GBP4 and IRF7 in Raw264.7 cells infected with SeV for 12 h. Data are representative of three independent experiments. Pre, preimmune serum.

GBP4 (Fig. 2*A*, 2*B*). To further confirm the endogenous interaction between GBP4 and IRF7, we induced expression of GBP4 and IRF7 by SeV infection for 12 h in Raw264.7 cells. Cell lysates were then subjected to immunoprecipitation analysis (Fig. 2*C*). The results show that endogenous GBP4 interacted with IRF7. These data indicate that the interaction of GBP4 with IRF7 may be involved in the regulation of SeV-induced ISRE signaling.

N terminus of GBP4 binds to the inhibitory domain of IRF7

To map the binding region between IRF7 and GBP4, a coimmunoprecipitation assay was performed with exogenous HA-tagged GBP4 and Flag-tagged deletion mutants of IRF7. The mutants without the inhibitory domain (Δ238-410) lost their affinity to GBP4 (Fig. 3*A*, 3*B*). However, binding abilities of GBP4 mutants were also detected (Fig. 3*C*, 3*D*). The mutants of GBP4 without an N terminal (GBP4-ΔN) lost their affinities to IRF7. In contrast, the deletion of the C terminal had no influence on the binding of GBP4 to IRF7. The results suggest that the N terminal of GBP4 and the inhibitory domain of IRF7 contribute to the interaction between GBP4 and IRF7.

GBP4 suppresses IRF7-dependent transcriptional activation

IRF7 has been identified as the master regulator of type I IFN production. Because we have demonstrated that GBP4 interacts with IRF7, we inquired whether GBP4 was able to regulate the transcriptional activity of IRF7. Reporter gene assays using a yeast transcription factor Gal4–IRF7 fusion protein showed that exogenous expression of GBP4 inhibited SeV induced IRF7-dependent transcriptional activation in a dose-dependent manner (Fig. 4*A*). Previous reports indicated that IRF7 has the ability to preferentially activate IFN-α production (26, 31). We then measured the IFN-α promoter activities in Hek293T. Because of the low ex-

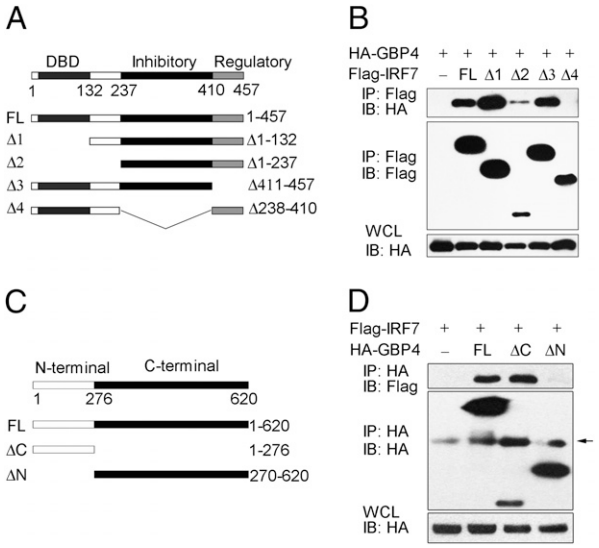

FIGURE 3. Identification of the domains required for the interaction between GBP4 and IRF7. *A* and *C*, A schematic presentation of IRF7 and GBP4 respectively. *B* and *D*, Hek293T cells were transfected with the indicated plasmids and coimmunoprecipitations were performed. Arrow indicates the H chains. Data are representative of three independent experiments. aa, amino acid.

pression of IRF7 in Hek293T, we cotransfected a small amount of IRF7 plasmid (1.0 ng), which was not sufficient for IFN-α promoter activation. As shown in Fig. 4*A*, exogenous expression of GBP4 inhibited SeV-induced activation of IFN-α4 promoter and IFN-α6 promoter. Under the same conditions, overexpression of GBP4 had no effect on SeV-induced activation of NF-κB promoter. Similarly, exogenous expression of GBP4 inhibited SeV-induced transcription activation of IRF7 in Raw264.7 (Fig. 4*B*). The GBP4 mutant GBP4-ΔN, which lacks the N terminal, did not efficiently inhibit SeV-induced IRF7-dependent transcriptional activation (Fig. 4*C*). It has been suggested that phosphorylation is central to the activation of IRF7 in response to viral infection through facilitating IRF7 translocation into the nucleus (32). We next addressed whether GBP4 affects virus-induced phosphorylation and nuclear translocation of IRF7. As reported previously (32), we found that SeV infection caused a shift of IRF7 in its electrophoretic mobility, which is indicative of protein phosphorylation (Fig. 4*D*). The phosphorylation of IRF7 was inhibited by exogenous expression of GBP4 (Fig. 4*D*). Consistent with the reporter assay (Fig. 4*C*), GBP4-ΔN had no effect on the phosphorylation of IRF7 (Fig. 4*D*). Accordingly, a significantly increased nuclear accumulation of IRF7 was observed after SeV infection (Fig. 4*E*). In the cells that were expressing GBP4, the SeV-triggered nuclear accumulation of IRF7 was suppressed, whereas NF-κB subunit p65 translocation was not affected (Fig. 4*E*). These data suggest that GBP4 efficiently inhibits IRF7-dependent transcriptional activation by downregulating virus-induced phosphorylation and nuclear accumulation of IRF7.

GBP4 inhibits TRAF6-induced IRF7 ubiquitination and transactivation

TRAF6-induced ubiquitination of IRF7 is a prerequisite for the phosphorylation of IRF7 that is induced by RLH signaling, and these processes are essential for nuclear retention by IRF7 and derepression of transactivation (33). Because the binding domain of IRF7 with GBP4 was the same as that of TRAF6 (33), we assumed that GBP4 could have potential for regulation of the activation of IRF7 by disrupting the interaction between TRAF6 and IRF7. To address this issue, we examined the effect of exogenous expression of GBP4 on the association of TRAF6 with

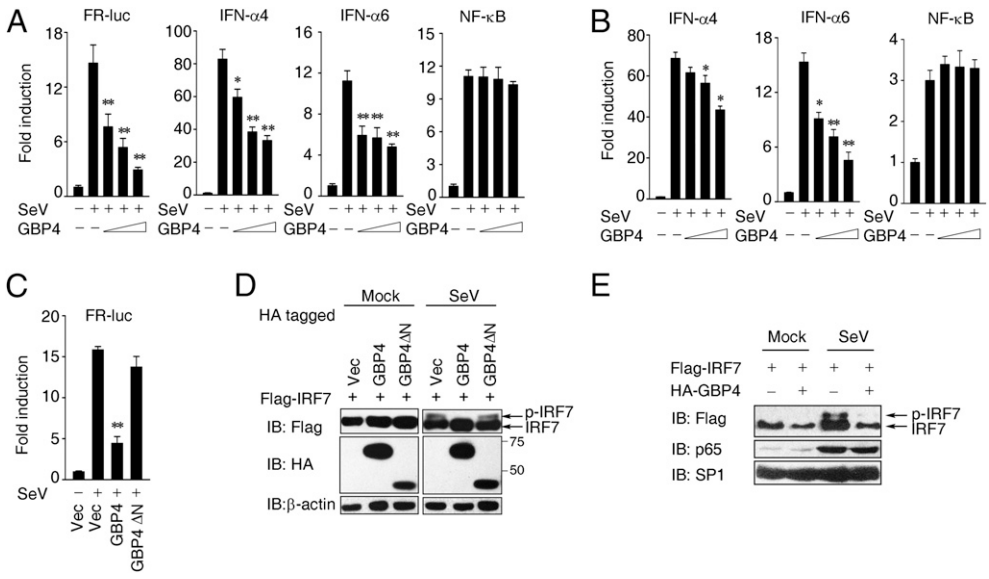

FIGURE 4. GBP4 suppresses virus induced activation of IRF7. Luciferase assay of lysates from Hek293T (*A*, *C*) or Raw264.7 (*B*) transfected with the indicated plasmids and then infected with SeV for 24 h. Results are presented as fold induction relative to cells without SeV infection. *A*, Hek293T were transfected with the GAL4 site luciferase reporter FR-luc (plus 1ng GAL4-IRF7), the IFN-α4 promoter (plus 1ng Flag-IRF7), the IFN-α6 promoter (plus 1 ng Flag-IRF7), the NF-κB promoter, and empty vector (−) or increased amounts of GBP4 (0.1, 0.2, and 0.4 μg). *B*, Raw264.7 cells were transfected with the IFN-α4 promoter (plus 1 ng Flag-IRF7), IFN-α6 promoter (plus 1 ng Flag-IRF7), or NF-κB promoter and empty vector (–) or increased amounts of GBP4 (0.1, 0.2, and 0.4 μg). *C*, Hek293T cells were transfected with the GAL4 site luciferase reporter FR-luc (plus 1 ng GAL4-IRF7) and indicated plasmids. *D*, Immunoblot of lysates of Hek293T transfected with Flag-IRF7 plus the indicated plasmids. After transfection, cells were treated with medium (control) or SeV for 12 h, and cell lysates were subjected to immunoblot with the indicated Ab. *E*, Nuclear extracts from SeV-infected 293T cells were monitored by immunoblotting for the appearance of IRF7, p65 subunit of NF-κB, and SP1 (loading control) in the nucleus. Luciferase activity is normalized to Renilla luciferase. Data are representative of three independent experiments. Results are presented as mean ± SD between duplicates ($n = 3$). *$p < 0.05$, **$p < 0.01$.

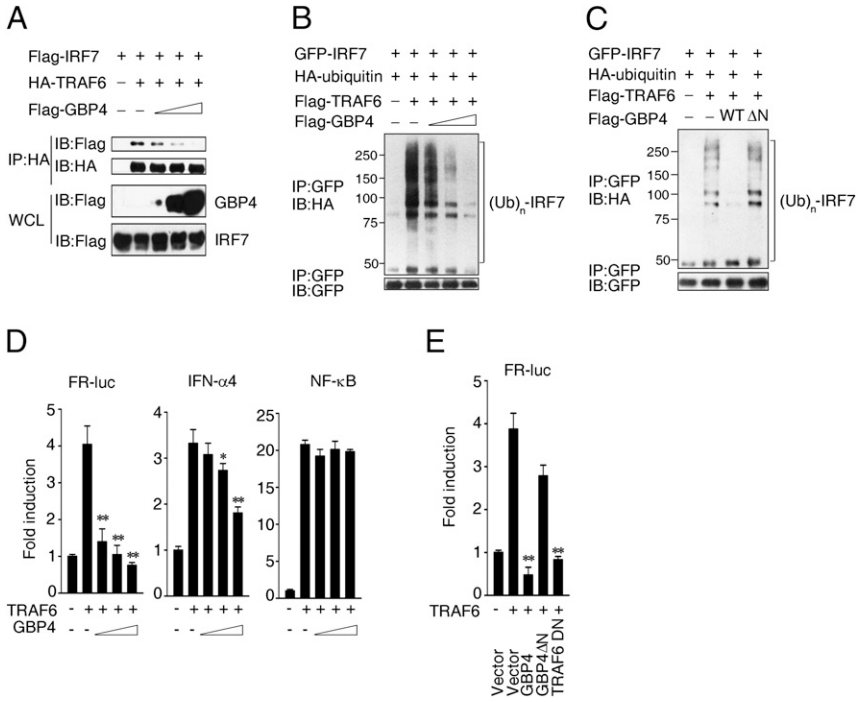

FIGURE 5. GBP4 inhibits TRAF6-induced ubiquitination and transactivation of IRF7. *A*, Hek293T cells were transfected with the indicated plasmids (1 μg each) and increasing amounts of GBP4 (0.5, 1, 2 μg). Coimmunoprecipitation and immunoblot analysis were performed. *B*, Hek293T cells were transfected with the indicated plasmids (0.5 μg GFP-IRF7, 0.1 μg HA-ubiquitin, 2 μg Flag-TRAF6) and increasing amounts of GBP4 (0.5, 1, and 2 μg). Immunoprecipitation and immunoblot analysis were performed. *C*, Hek293T cells were transfected with the indicated plasmids. Immunoprecipitation and immunoblot analysis were performed. *D*, Luciferase assay of lysates from Hek293T cells transfected with empty vector (−) or TRAF6 plus GAL4 site luciferase reporter FR-luc (plus 1 ng GAL4-IRF7), or promoter IFN-α4 (plus 1 ng Flag-IRF7) or promoter NF-κB, and empty vector (−) or increased amounts of GBP4 (0.1, 0.2, and 0.4 μg). Results are presented as fold induction relative to cells with no TRAF6 transfection. *E*, Luciferase assay of lysates from Hek293T cells transfected with empty vector (−) or TRAF6 plus GAL4 site luciferase reporter FR-luc (plus 1 ng GAL4-IRF7), plus the indicated plasmids. Data are representative of three independent experiments. Results are presented as fold induction relative to cells with no TRAF6 transfection.

IRF7 by competitive coimmunoprecipitation. The results show that GBP4 was able to disrupt the interaction of TRAF6 and IRF7 in a dose-dependent manner (Fig. 5*A*). We next tested whether GBP4 was able to regulate TRAF6-induced ubiquitination of IRF7. We transiently transfected HEK293T cells with GFP-IRF7 and HA-ubiquitin with or without Flag-TRAF6 and then immunoprecipitated proteins with anti-GFP, followed by immunoblotting with anti-HA. Slowly migrating forms of GFP-IRF7 were strongly induced by TRAF6 overexpression (Fig. 5*B*), indicating that TRAF6 induced a remarkable ubiquitination of IRF7. As predicted, exogenous expression of GBP4 inhibited the TRAF6 induced ubiquitination of IRF7, but expression of GBP4-ΔN did not (Fig. 5*B*, 5*C*). Reduction of the ubiquitination of IRF7 led to impaired transactivation ability of IRF7 (34). Therefore, we assumed that overexpression of GBP4 could inhibit TRAF6-induced IRF7 transactivation. The reporter gene assays showed that overexpression of GBP4 inhibited TRAF6-induced IRF7-dependent transcriptional activation (Fig. 5*D*), while the inhibition was abolished by deletion of the N terminus of GBP4 (Fig. 5*E*), suggesting that the interaction between GBP4 and IRF7 is critical for the regulatory effect of GBP4. As a positive control, the dominant negative mutant of TRAF6 was used to inhibit TRAF6-induced IRF7 transcriptional activation (Fig. 5*E*). These data indicate that GBP4 inhibits TRAF6-induced ubiquitination and transcriptional activation of IRF7 by disrupting the association of TRAF6 and IRF7.

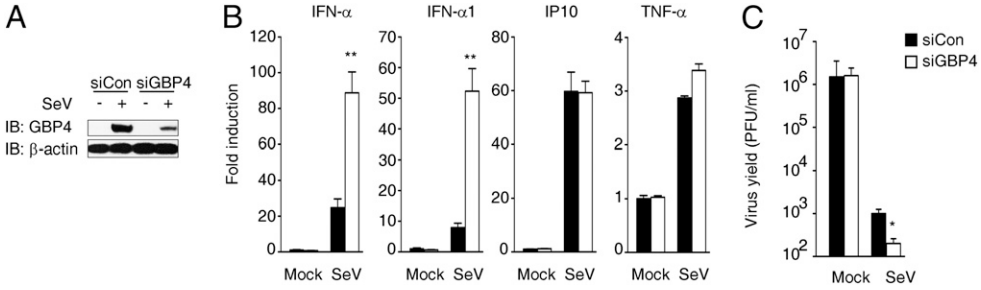

FIGURE 6. Endogenous GBP4 negatively regulates IRF7-dependent transcriptional activation of IFN-α and antiviral response. *A*, Knockdown of GBP4 by siRNA. After transfection with control siRNA or GBP4 siRNA, Raw264.7 cells were treated with medium or SeV for 12 h, and the cell lysates were subjected to immunoblot analysis with anti-GBP4 or anti–β-actin (loading control) to detect knockdown efficiency. *B*, Real-time PCR analysis of expression levels of IFN-α, IFN-α1, IP10, and TNF-α in Raw264.7 treated as described in *A*. *C*, IFN bioassay of conditioned media from siRNA transfected Raw264.7 infected with SeV for 24 h. Data are representative of three independent experiments. Data are presented as mean ± SD between duplicates (n = 3). *$p < 0.05$.

Endogenous GBP4 negatively regulates IRF7-mediated signaling and antiviral response

To determine whether GBP4 is involved in the regulation of IRF7-mediated IFN-α production under physiologic conditions, we examined the effects of knockdown of GBP4 on virus-triggered signaling. We found that GBP4 siRNA efficiently inhibited the expression of endogenous GBP4 in Raw264.7 compared with control siRNA (Fig. 6*A*). Real-time PCR analysis showed that knockdown of GBP4 significantly increased the level of total IFN-α and IFN-α1 triggered by SeV infection, whereas expression levels of IP-10 and TNF-α were not altered (Fig. 6*B*). Consistently, GBP4 silencing in RAW264.7 significantly increased SeV-induced IFN-α at the protein level as determined by ELISA, whereas expression levels of TNF-α were not altered (Supplemental Fig. 3). Furthermore, similar results were obtained in BMDCs (Supplemental Fig. 4). The results suggest that GBP4 is largely involved in regulation of IRF7-dependent transcription activities. Moreover, culture supernatants from SeV-infected cells were tested for IFN activity by using a bioassay that measures the ability of IFN to block replication of VSV. The supernatant from GBP4 knockdown Raw264.7 cells infected with SeV inhibited VSV replication more efficiently than the supernatant collected from control siRNA transfected cells (Fig. 6*C*). The data indicate that there was more IFN secreted from the GBP4 knockdown cells, which is consistent with the results of real-time PCR. Our results suggest that GBP4 is a negative regulator of cellular antiviral response through the targeting of IRF7-dependent IFN-α production.

Discussion

In this study, we have identified GBP4 as a novel negative regulator of RLH-mediated activation of IRF7. Knockdown of endogenous GBP4 increased IRF7-mediated IFN-α production, whereas overexpression of GBP4 had the opposite effect. Our results demonstrate that GBP4 achieves these effects by disrupting interaction of TRAF6 and IRF7, thus inhibiting IRF7 ubiquitination and virus induced phosphorylation.

Aberrant production of IFN is associated with many types of disease, such as cancers, immune disorders, and multiple sclerosis (35–39). To prevent harmful effects of excessive production of type I IFN, the virus-triggered signaling must be tightly regulated. Several mechanisms are proven to underlie the tight regulation of RIG-I signaling. A number of molecules, including RNF125, A20, DUBA, Pin1, NLRX1, SIKE, DAK, RNF5, ISG56, and Triad3A, have been shown to target distinct components of the virus-triggered signaling pathways maintaining physiologic processes (40–43). However, as the central regulator of production of type I IFNs, little is known about the regulation of IRF7 activity except by several viral proteins (44–46). For example, ORF45, a Kaposi sarcoma-associated herpesvirus immediate-early protein, blocks IRF7 phosphorylation and nuclear accumulation induced by virus infection. BZLF-1 inhibits activation of IRF7 triggered by LMP1 or polyinosinic-polycytidylic acid. RTA, also an immediate-early nuclear transcription factor encoded by Kaposi sarcoma-associated herpesvirus, promotes the ubiquitination and degradation of IRF7. In this study, we demonstrate that GBP4, highly induced by SeV, is a negative regulator of activation of IRF7, inhibiting SeV-triggered phosphorylation and nuclear accumulation of IRF7.

It is believed that activation of IRF7 is regulated by its phosphorylation (32). Several kinases, including TBK1, IKKi, inhibitor of NF-κB kinase-α, and IRAK1, are involved in the phosphorylation of IRF7 (47–50). The phosphorylation unmasks a binding domain of IRF7, as well as leading to the formation of a homodimer or heterodimer with IRF3, subsequently allowing translocation into the nucleus and binding to a specific DNA sequence for induction of target gene expression. In our study, we found that overexpression of GBP4 inhibited SeV-induced phosphorylation and nuclear accumulation of IRF7.

TRAF6 associates with and activates IRF7 in both TLRs (TLR7/8 and TLR9) and RLH signaling pathways. TRAF6 functions as an E3 ligase together with a ubiquitin-conjugating enzyme complex that catalyzes the synthesis of polyubiquitin linked to lysine 63 of ubiquitin. Lysine 63-mediated ubiquitination of IRF7 by TRAF6 is required for full activation of IRF7 (26, 34). Mutation of the major ubiquitination sites at the C-terminal of IRF7 results in consistent decreases in ubiquitination intensity and abrogates the transactivation ability of IRF7 (34). This finding was confirmed by the observation of TRAF6-deficient mouse embryonic fibroblast which showed reduced ubiquitination of IRF7 in the presence of LMP1. Moreover, impaired phosphorylation of IRF7 was observed in TRAF6-deficient mouse embryonic fibroblast cells after polyinosinic-polycytidylic acid transfection or B-DNA stimulation, implying that regulatory ubiquitination of IRF7 is a prelude to its phosphorylation (33). These observations suggest that K63-linked ubiquitination of IRF7 is likely to be a widespread mechanism triggered by a variety of infections. In this study, based on competitive coimmunoprecipitation experiments, we demonstrate that GBP4 disrupts the TRAF6 and IRF7 interactions and inhibits TRAF6-induced ubiquitination of IRF7. Consistently, SeV-induced phosphorylation and transactivation of IRF7 were suppressed by overexpression of GBP4 but not GBP4-ΔN, which lost its affinity to IRF7. Thus, our data identify a new regulatory mechanism for modulating the activation of IRF7.

Our results demonstrate that GBP4 targets IRF7 to inhibit its transactivation. The overall function of this process is to turn off or limit the excess production of IFN-α. Thus we report a novel role for GBP4 in regulating cellular antiviral responses.

Acknowledgments

We thank Prof. Takashi Fuijita and Chen Wang for providing regents for the study, Prof. Hongbing Shu and Genhong Cheng for providing regents and instructive suggestions, and Dr. Sheri Skinner for reviewing the manuscript.

Disclosures

The authors have no financial conflicts of interest.

References

1. Kawai, T., and S. Akira. 2010. The role of pattern-recognition receptors in innate immunity: update on Toll-like receptors. *Nat. Immunol.* 11: 373–384.
2. O'Neill, L. A., and A. G. Bowie. 2010. Sensing and signaling in antiviral innate immunity. *Curr. Biol.* 20: R328–R333.
3. Wilkins, C., and M. Gale, Jr. 2010. Recognition of viruses by cytoplasmic sensors. *Curr. Opin. Immunol.* 22: 41–47.
4. Kawai, T., and S. Akira. 2008. Toll-like receptor and RIG-I-like receptor signaling. *Ann. N. Y. Acad. Sci.* 1143: 1–20.
5. Akira, S., S. Uematsu, and O. Takeuchi. 2006. Pathogen recognition and innate immunity. *Cell* 124: 783–801.
6. Lund, J. M., L. Alexopoulou, A. Sato, M. Karow, N. C. Adams, N. W. Gale, A. Iwasaki, and R. A. Flavell. 2004. Recognition of single-stranded RNA viruses by Toll-like receptor 7. *Proc. Natl. Acad. Sci. USA* 101: 5598–5603.
7. Diebold, S. S., T. Kaisho, H. Hemmi, S. Akira, and C. Reis e Sousa. 2004. Innate antiviral responses by means of TLR7-mediated recognition of single-stranded RNA. *Science* 303: 1529–1531.
8. Krug, A., G. D. Luker, W. Barchet, D. A. Leib, S. Akira, and M. Colonna. 2004. Herpes simplex virus type 1 activates murine natural interferon-producing cells through toll-like receptor 9. *Blood* 103: 1433–1437.
9. Krug, A., A. R. French, W. Barchet, J. A. Fischer, A. Dzionek, J. T. Pingel, M. M. Orihuela, S. Akira, W. M. Yokoyama, and M. Colonna. 2004. TLR9-dependent recognition of MCMV by IPC and DC generates coordinated cytokine responses that activate antiviral NK cell function. *Immunity* 21: 107–119.
10. Lund, J., A. Sato, S. Akira, R. Medzhitov, and A. Iwasaki. 2003. Toll-like receptor 9-mediated recognition of Herpes simplex virus-2 by plasmacytoid dendritic cells. *J. Exp. Med.* 198: 513–520.

11. Yoneyama, M., M. Kikuchi, T. Natsukawa, N. Shinobu, T. Imaizumi, M. Miyagishi, K. Taira, S. Akira, and T. Fujita. 2004. The RNA helicase RIG-I has an essential function in double-stranded RNA-induced innate antiviral responses. *Nat. Immunol.* 5: 730–737.
12. Andrejeva, J., K. S. Childs, D. F. Young, T. S. Carlos, N. Stock, S. Goodbourn, and R. E. Randall. 2004. The V proteins of paramyxoviruses bind the IFN-inducible RNA helicase, mda-5, and inhibit its activation of the IFN-beta promoter. *Proc. Natl. Acad. Sci. USA* 101: 17264–17269.
13. Yoneyama, M., and T. Fujita. 2009. RNA recognition and signal transduction by RIG-I-like receptors. *Immunol. Rev.* 227: 54–65.
14. Lei, Y., C. B. Moore, R. M. Liesman, B. P. O'Connor, D. T. Bergstralh, Z. J. Chen, R. J. Pickles, and J. P. Ting. 2009. MAVS-mediated apoptosis and its inhibition by viral proteins. *PLoS ONE* 4: e5466.
15. Honda, K., H. Yanai, H. Negishi, M. Asagiri, M. Sato, T. Mizutani, N. Shimada, Y. Ohba, A. Takaoka, N. Yoshida, and T. Taniguchi. 2005. IRF-7 is the master regulator of type-I interferon-dependent immune responses. *Nature* 434: 772–777.
16. Zhang, M., Y. Tian, R. P. Wang, D. Gao, Y. Zhang, F. C. Diao, D. Y. Chen, Z. H. Zhai, and H. B. Shu. 2008. Negative feedback regulation of cellular antiviral signaling by RBCK1-mediated degradation of IRF3. *Cell Res.* 18: 1096–1104.
17. Saitoh, T., M. Yamamoto, M. Miyagishi, K. Taira, M. Nakanishi, T. Fujita, S. Akira, N. Yamamoto, and S. Yamaoka. 2005. A20 is a negative regulator of IFN regulatory factor 3 signaling. *J. Immunol.* 174: 1507–1512.
18. Saitoh, T., A. Tun-Kyi, A. Ryo, M. Yamamoto, G. Finn, T. Fujita, S. Akira, N. Yamamoto, K. P. Lu, and S. Yamaoka. 2006. Negative regulation of interferon-regulatory factor 3-dependent innate antiviral response by the prolyl isomerase Pin1. *Nat. Immunol.* 7: 598–605.
19. Higgs, R., J. Ní Gabhann, N. Ben Larbi, E. P. Breen, K. A. Fitzgerald, and C. A. Jefferies. 2008. The E3 ubiquitin ligase Ro52 negatively regulates IFN-beta production post-pathogen recognition by polyubiquitin-mediated degradation of IRF3. *J. Immunol.* 181: 1780–1786.
20. Martens, S., and J. Howard. 2006. The interferon-inducible GTPases. *Annu. Rev. Cell Dev. Biol.* 22: 559–589.
21. MacMicking, J. D. 2004. IFN-inducible GTPases and immunity to intracellular pathogens. *Trends Immunol.* 25: 601–609.
22. Shenoy, A. R., B. H. Kim, H. P. Choi, T. Matsuzawa, S. Tiwari, and J. D. MacMicking. 2007. Emerging themes in IFN-gamma-induced macrophage immunity by the p47 and p65 GTPase families. *Immunobiology* 212: 771–784.
23. Itsui, Y., N. Sakamoto, S. Kakinuma, M. Nakagawa, Y. Sekine-Osajima, M. Tasaka-Fujita, Y. Nishimura-Sakurai, G. Suda, Y. Karakama, K. Mishima, et al. 2009. Antiviral effects of the interferon-induced protein guanylate binding protein 1 and its interaction with the hepatitis C virus NS5B protein. *Hepatology* 50: 1727–1737.
24. Anderson, S. L., J. M. Carton, J. Lou, L. Xing, and B. Y. Rubin. 1999. Interferon-induced guanylate binding protein-1 (GBP-1) mediates an antiviral effect against vesicular stomatitis virus and encephalomyocarditis virus. *Virology* 256: 8–14.
25. Carter, C. C., V. Y. Gorbacheva, and D. J. Vestal. 2005. Inhibition of VSV and EMCV replication by the interferon-induced GTPase, mGBP-2: differential requirement for wild-type GTP binding domain. *Arch. Virol.* 150: 1213–1220.
26. Kawai, T., S. Sato, K. J. Ishii, C. Coban, H. Hemmi, M. Yamamoto, K. Terai M. Matsuda, J. Inoue, S. Uematsu, et al. 2004. Interferon-alpha induction through Toll-like receptors involves a direct interaction of IRF7 with MyD88 and TRAF6. *Nat. Immunol.* 5: 1061–1068.
27. Shi, M., W. Deng, E. Bi, K. Mao, Y. Ji, G. Lin, X. Wu, Z. Tao, Z. Li, X. Cai, et al. 2008. TRIM30 alpha negatively regulates TLR-mediated NF-kappa B activation by targeting TAB2 and TAB3 for degradation. *Nat. Immunol.* 9: 369–377.
28. Hou, W., Y. Wu, S. Sun, M. Shi, Y. Sun, C. Yang, G. Pei, Y. Gu, C. Zhong, and B. Sun. 2003. Pertussis toxin enhances Th1 responses by stimulation of dendritic cells. *J. Immunol.* 170: 1728–1736.
29. Huang, C., E. Bi, Y. Hu, W. Deng, Z. Tian, C. Dong, Y. Hu, and B. Sun. 2006. A novel NF-kappaB binding site controls human granzyme B gene transcription. *J. Immunol.* 176: 4173–4181.
30. Friedman, C. S., M. A. O'Donnell, D. Legarda-Addison, A. Ng, W. B. Cárdenas, J. S. Yount, T. M. Moran, C. F. Basler, A. Komuro, C. M. Horvath, et al. 2008. The tumour suppressor CYLD is a negative regulator of RIG-I-mediated antiviral response. *EMBO Rep.* 9: 930–936.
31. Steinberg, C., K. Eisenächer, O. Gross, W. Reindl, F. Schmitz, J. Ruland, and A. Krug. 2009. The IFN regulatory factor 7-dependent type I IFN response is not essential for early resistance against murine cytomegalovirus infection. *Eur. J. Immunol.* 39: 1007–1018.
32. Marié, I., E. Smith, A. Prakash, and D. E. Levy. 2000. Phosphorylation-induced dimerization of interferon regulatory factor 7 unmasks DNA binding and a bipartite transactivation domain. *Mol. Cell. Biol.* 20: 8803–8814.
33. Konno, H., T. Yamamoto, K. Yamazaki, J. Gohda, T. Akiyama, K. Semba, H. Goto, A. Kato, T. Yujiri, T. Imai, et al. 2009. TRAF6 establishes innate immune responses by activating NF-kappaB and IRF7 upon sensing cytosolic viral RNA and DNA. *PLoS ONE* 4: e5674.
34. Ning, S., A. D. Campos, B. G. Darnay, G. L. Bentz, and J. S. Pagano. 2008. TRAF6 and the three C-terminal lysine sites on IRF7 are required for its ubiquitination-mediated activation by the tumor necrosis factor receptor family member latent membrane protein 1. *Mol. Cell. Biol.* 28: 6536–6546.
35. Salloum, R., B. S. Franek, S. N. Kariuki, L. Rhee, R. A. Mikolaitis, M. Jolly, T. O. Utset, and T. B. Niewold. 2010. Genetic variation at the IRF7/PHRF1 locus is associated with autoantibody profile and serum interferon-alpha activity in lupus patients. *Arthritis Rheum.* 62: 553–561.
36. Stetson, D. B., and R. Medzhitov. 2006. Type I interferons in host defense. *Immunity* 25: 373–381.
37. Bonjardim, C. A., P. C. Ferreira, and E. G. Kroon. 2009. Interferons: signaling, antiviral and viral evasion. *Immunol. Lett.* 122: 1–11.
38. Borden, E. C., G. C. Sen, G. Uze, R. H. Silverman, R. M. Ransohoff, G. R. Foster, and G. R. Stark. 2007. Interferons at age 50: past, current and future impact on biomedicine. *Nat. Rev. Drug Discov.* 6: 975–990.
39. Wada, M., H. Marusawa, R. Yamada, A. Nasu, Y. Osaki, M. Kudo, M. Nabeshima, Y. Fukuda, T. Chiba, and F. Matsuda. 2009. Association of genetic polymorphisms with interferon-induced haematologic adverse effects in chronic hepatitis C patients. *J. Viral Hepat.* 16: 388–396.
40. Zhong, B., L. Zhang, C. Lei, Y. Li, A. P. Mao, Y. Yang, Y. Y. Wang, X. L. Zhang, and H. B. Shu. 2009. The ubiquitin ligase RNF5 regulates antiviral responses by mediating degradation of the adaptor protein MITA. *Immunity* 30: 397–407.
41. Takeuchi, O., and S. Akira. 2009. Innate immunity to virus infection. *Immunol. Rev.* 227: 75–86.
42. Nakhaei, P., T. Mesplede, M. Solis, Q. Sun, T. Zhao, L. Yang, T. H. Chuang, C. F. Ware, R. Lin, and J. Hiscott. 2009. The E3 ubiquitin ligase Triad3A negatively regulates the RIG-I/MAVS signaling pathway by targeting TRAF3 for degradation. *PLoS Pathog.* 5: e1000650.
43. Li, Y., C. Li, P. Xue, B. Zhong, A. P. Mao, Y. Ran, H. Chen, Y. Y. Wang, F. Yang, and H. B. Shu. 2009. ISG56 is a negative-feedback regulator of virus-triggered signaling and cellular antiviral response. *Proc. Natl. Acad. Sci. USA* 106: 7945–7950.
44. Yu, Y., S. E. Wang, and G. S. Hayward. 2005. The KSHV immediate-early transcription factor RTA encodes ubiquitin E3 ligase activity that targets IRF7 for proteosome-mediated degradation. *Immunity* 22: 59–70.
45. Hahn, A. M., L. E. Huye, S. Ning, J. Webster-Cyriaque, and J. S. Pagano. 2005. Interferon regulatory factor 7 is negatively regulated by the Epstein-Barr virus immediate-early gene, BZLF-1. *J. Virol.* 79: 10040–10052.
46. Zhu, F. X., S. M. King, E. J. Smith, D. E. Levy, and Y. Yuan. 2002. A Kaposi's sarcoma-associated herpesviral protein inhibits virus-mediated induction of type I interferon by blocking IRF-7 phosphorylation and nuclear accumulation. *Proc. Natl. Acad. Sci. USA* 99: 5573–5578.
47. Uematsu, S., S. Sato, M. Yamamoto, T. Hirotani, H. Kato, F. Takeshita, M. Matsuda, C. Coban, K. J. Ishii, T. Kawai, et al. 2005. Interleukin-1 receptor-associated kinase-1 plays an essential role for Toll-like receptor (TLR)7- and TLR9-mediated interferon-alpha induction. *J. Exp. Med.* 201: 915–923.
48. Fitzgerald, K. A., S. M. McWhirter, K. L. Faia, D. C. Rowe, E. Latz, D. T. Golenbock, A. J. Coyle, S. M. Liao, and T. Maniatis. 2003. IKKepsilon and TBK1 are essential components of the IRF3 signaling pathway. *Nat. Immunol.* 4: 491–496.
49. Hoshino, K., T. Sugiyama, M. Matsumoto, T. Tanaka, M. Saito, H. Hemmi, O. Ohara, S. Akira, and T. Kaisho. 2006. IkappaB kinase-alpha is critical for interferon-alpha production induced by Toll-like receptors 7 and 9. *Nature* 440: 949–953.
50. Sharma, S., B. R. tenOever, N. Grandvaux, G. P. Zhou, R. Lin, and J. Hiscott. 2003. Triggering the interferon antiviral response through an IKK-related pathway. *Science* 300: 1148–1151.